

## ARTICLE

# All-atom Molecular Dynamics Simulations and NMR Spectroscopy Study on Interactions and Structures in *N*-Glycylglycine Aqueous Solution

Rong Zhang\*, Wen-juan Wu, Jing-man Huang, Xin Meng

Laboratory of Physical Chemistry, College of Pharmacy, Guangdong Pharmaceutical University, Guangzhou 510006, China

(Dated: Received on June 19, 2011; Accepted on August 5, 2011)

All-atom molecular dynamics (MD) simulation and the NMR spectra are used to investigate the interactions in *N*-glycylglycine aqueous solution. Different types of atoms exhibit different capability in forming hydrogen bonds by the radial distribution function analysis. Some typical dominant aggregates are found in different types of hydrogen bonds by the statistical hydrogen-bonding network. Moreover, temperature-dependent NMR are used to compare with the results of the MD simulations. The chemical shifts of the three hydrogen atoms all decrease with the temperature increasing which reveals that the hydrogen bonds are dominant in the glycylglycine aqueous solution. And the NMR results show agreement with the MD simulations. All-atom MD simulations and NMR spectra are successful in revealing the structures and interactions in the *N*-glycylglycine-water mixtures.

**Key words:** All-atom simulation, Temperature-dependent NMR, *N*-glycylglycine aqueous solution, Hydrogen bond

## I. INTRODUCTION

Interactions between the peptide groups play an essential role in the structures and properties of proteins and nucleic acids as well as in the behavior of many solvent systems [1–3]. Some model peptide and simple peptide systems have been investigated extensively as the models of peptide bonds because of its presence as a repeating unit in biological macromolecules and some polymers [4–8]. Recently, it is recognized that weak contacts such as C–H···O exist widely in important biological systems as nucleic acids, proteins and carbohydrates, which may be the key to protein folding. The C–H···O interactions play a significant role in determining the molecular conformation, stabilization of complexes and in the activity of biological macromolecules [9, 10].

Molecular dynamics (MD) simulation has been proven to be particularly valuable for studying structures and interactions in the biomolecular system [11–13]. Spectral measurements such as NMR spectra are highly powerful techniques which can be used to investigate structures and interactions in the mixtures [14–16]. A variety of experimental and theoretical methods have been carried out to study the *N*-glycylglycine [17–21]. Wang and co-workers used flow microcalorimetry to investigate enthalpies of dilution of *N*-glycylglycine in aqueous sodium chloride

and potassium chloride solutions [18]. It was found that the enthalpic pairwise interaction coefficients of *N*-glycylglycine in both electrolyte solutions are negative. The results were discussed in terms of the solute-solute and solute-solvent interactions. Pajcini and co-workers adopted near-resonance Raman single-crystal measurements to determine the orientation of the transition moments of the resonant excited state and the next closest excited state of the glycylglycine [20]. They found that these transition moment orientations occurred for a glycylglycine crystal where the carboxylates were hydrated and the amide groups were hydrogen-bonded in a  $\beta$ -sheet like structure.

We have investigated the interactions and structures in the special associate system such as amide-water mixtures [6, 22–24]. Some interesting phenomena were observed in the mixtures, for instance, the two methyl groups in amide molecule are found to show different capabilities in forming weak C–H···O contacts in the mixtures from the radial distribution functions (RDFs). Furthermore, the temperature-dependent NMR results of the different methyl groups also show excellent agreements with the MD simulations.

In the present work, we used an all-atom MD simulation and NMR spectra to investigate the intermolecular interactions in the *N*-glycylglycine aqueous solution. The structure of *N*-glycylglycine is shown in Fig.1. The RDFs, the statistics of hydrogen bonding networks and temperature-dependent NMR were used to reveal the interactions and structures in the glycylglycine aqueous solutions. The results provided a qualitative description of glycylglycine-water mixtures.

\* Author to whom correspondence should be addressed. E-mail: zhangr@china.com.cn

## II. CALCULATION

### A. Molecular models

Simple potential models were used for glycylglycine and water. The nonbonded interactions are represented by a sum of the Coulomb and Lennard-Jones terms with Eq.(1)

$$E_{ab} = \sum_i^{\text{on a}} \sum_j^{\text{on b}} \left[ \frac{q_i q_j e^2}{r_{ij}} + 4\epsilon_{ij} \left( \frac{\sigma_{ij}^{12}}{r_{ij}^{12}} - \frac{\sigma_{ij}^6}{r_{ij}^6} \right) \right] f_{ij} \quad (1)$$

where  $E_{ab}$  is the interaction energy between molecules a and b. Standard combining rules are used via Eq.(2).

$$\begin{aligned} \sigma_{ij} &= \sqrt{\sigma_{ii}\sigma_{jj}} \\ \epsilon_{ij} &= \sqrt{\epsilon_{ii}\epsilon_{jj}} \end{aligned} \quad (2)$$

The same expression is used for intramolecular non-bonded interactions between all pairs of atoms ( $i < j$ ) separated by three or more bonds. In Eq.(1),  $f_{ij}=1.0$  except for intramolecular 1,4 interactions for which  $f_{ij}=0.5$ .

Simple point charge (SPC) model [25] and optimized potentials for liquid simulations-all atom (OPLS-AA) [26, 27] model are used for water and glycylglycine molecules which are shown in Table I. The glycylglycine molecule are ionized in the aqueous solution, and mainly keep the charged state in the neutral solution, and the properties of this charged state are the greatest important under physiological conditions. The structure of glycylglycine is shown in Fig.1.

### B. Simulation detail

MD calculations were performed by a modified TINKER 4.2 molecular modeling package [28]. The simulations were carried out in the NPT ensemble at  $T=298$  K and  $P=100$  kPa with a total of 768 molecules. Concentration of glycylglycine molecules are at 0.145, 0.364, 0.659, 0.807, and 1.013 mol/L. Periodical boundary conditions were used together with a sphere cutoff. The SHAKE algorithm was applied to constrain the bond length of the glycylglycine molecules, and the SETTLE algorithm was used to constrain the water geometry. The energies of the initial configurations were minimized using the MINIMIZE program in the TINKER 4.2 package. The time step was 1 fs and the configurations were saved every 0.1 ps for analysis. The mixtures were sufficiently equilibrated to ensure that there were no systematic drifts in the potential energies with time. The equilibrations were followed by monitoring the RDFs as well as the fraction of molecules of each species that had a given number of hydrogen bonds. The statistics were collected during the last 1 fs.

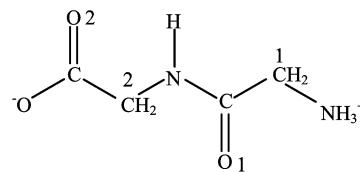


FIG. 1 Structure of *N*-glycylglycine molecule. The numbers denote different type atoms in *N*-glycylglycine molecules.

TABLE I Potential parameters and symbol of the atoms for SPC water and glycylglycine.

Atom	$\sigma/\text{\AA}$	$\epsilon/(\text{kJ/mol})$	$q/e$
SPC water			
O <sub>W</sub>	3.1656	0.1554	-0.8200
H <sub>W</sub>	0.0000	0.0000	0.4100
Glycylglycine			
C1 (CH <sub>2</sub> )	3.5000	0.0660	-0.1800
C2 (CH <sub>2</sub> )	3.5000	0.0660	-0.1800
C3 (C=O)	3.7500	0.1050	0.5000
O1 (C=O)	2.9600	0.2100	-0.5000
C4 (COO <sup>-</sup> )	3.7500	0.1050	0.7000
O2 (COO <sup>-</sup> )	2.9600	0.2100	-0.8000
N1 (NH <sub>3</sub> <sup>+</sup> )	3.2500	0.1700	-0.3000
N2 (NH)	3.2500	0.1700	-0.5000
H <sub>C1</sub> (CH <sub>2</sub> )	2.5000	0.0300	0.0600
H <sub>C2</sub> (CH <sub>2</sub> )	2.5000	0.0300	0.0600
H <sub>N1</sub> (NH <sub>3</sub> <sup>+</sup> )	0.0000	0.0000	0.3300
H <sub>N2</sub> (NH)	0.0000	0.0000	0.3000

### C. Definition

An analysis of hydrogen bonding networks was used to gain deeper insight into the aqueous structures. Here a geometric criterion that is the same as that used by Luzar and Chandler has been performed [29], such as a typical criteria of neat water:  $R(\text{O}_W \cdots \text{H}_W) \leq 2.45$  Å,  $R(\text{O}_W \cdots \text{O}_W) \leq 3.60$  Å, and the angle  $\angle \text{H}_W - \text{O}_W \cdots \text{O}_W \leq 30^\circ$ . where O<sub>W</sub> refers to oxygen atoms of water and H<sub>W</sub> refers to hydrogen atom.

## III. EXPERIMENTS

NMR spectrum is highly powerful techniques which can be used to investigate structures and interactions in the mixtures. NMR spectra were measured using a Bruker DMX 500 spectrometer operating at 500 MHz at different temperatures with an accuracy of  $\pm 0.1$  °C. The solution was 90% H<sub>2</sub>O/10% D<sub>2</sub>O samples which were typically used in biological NMR to make the signal of the active proton appear in the spectra [30–32]. The chemical shifts for <sup>1</sup>H atom of glycylglycine-water mixtures at temperatures of 298, 308, 318, and 328 K were measured.

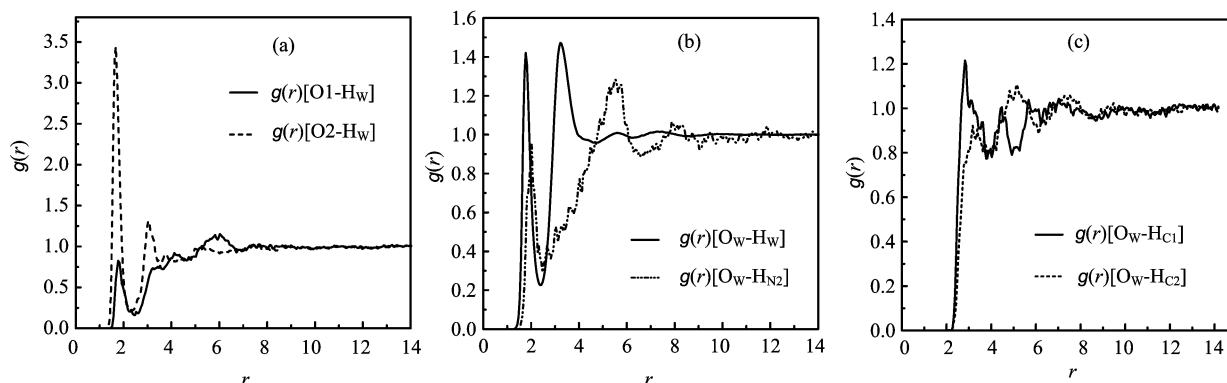


FIG. 2 RDF in the glycylglycine-water mixtures (0.145 mol/L).

## IV. RESULTS AND DISCUSSION

### A. $g(r)$ in the glycylglycine-water system

The structure of the liquid can be characterized well by the RDF,  $g(r)[x-y]$ , which gives the probability of finding an atom of type  $y$  at a distance  $r$  from an atom of type  $x$ . The  $g(r)$ s that concern intermolecular interactions at the concentration of 0.145 mol/L are given in Fig.2. The distinct peaks near 1.8 Å are both observed in  $g(r)[O1-H_W]$  and  $g(r)[O2-H_W]$  shown in Fig.2(a) which implies that there exist traditional  $C=O \cdots H_W$  hydrogen bonds in the solution. Interestingly, the intensity of  $g(r)[O2-H_W]$  is much larger than that of  $g(r)[O1-H_W]$ . The distance of the first peak of  $g(r)[O2-H_W]$  (1.7 Å) is shorter than that of  $g(r)[O1-H_W]$  (1.8 Å). The shorter distances and stronger intensities exhibit that the capabilities in forming the  $C=O2 \cdots H_W$  hydrogen bonds are stronger than those of  $C=O1 \cdots H_W$ . The traditional  $O_W-H_W \cdots O_W$  and  $N-H \cdots O_W$  hydrogen bonds also play an important role in the solution. The obvious peaks of the second hydration shell are observed near 3 Å in  $g(r)[O1-H_W]$  which implies that the across-associate aggregates of the atoms O1 and  $H_W$  are more structured. Comparison between the  $g(r)[O_W-H_W]$  and  $g(r)[O_W-H_{N2}]$  are shown in Fig.2(b). The  $g(r)[O_W-H_W]$  presents two distinct peaks near 1.8, and 3.2 Å. For  $g(r)[O_W-H_{N2}]$ , the two peaks appears near 2.0 and 5.5 Å. The intensities of the two peaks in  $g(r)[O_W-H_W]$  are larger than those of  $g(r)[O_W-H_{N2}]$ . The stronger intensities and shorter distances imply that the capabilities in forming the  $O_W-H_W \cdots O_W$  hydrogen bonds are stronger than those of  $N-H \cdots O_W$ . The oxygen atoms of water ( $O_W$ ) prefer its own hydrogen atom ( $H_W$ ) as acceptors. The obvious second peaks of the second hydration shell near 3.2 Å in  $g(r)[O_W-H_W]$  also shows that there are the stable aggregates of the water molecules in the solutions. The  $g(r)[O_W-H_{C1}]$  presents three distinct peaks near 2.8, 4.4, and 5.8 Å, respectively shown in Fig.2(c). Interestingly, the first peak of  $g(r)[O-H_{C2}]$  is 3.1 Å which is larger than that of  $g(r)[O_W-H_{C1}]$ .

Also, the intensity of the first peak in  $g(r)[O_W-H_{C1}]$  is weaker than that of  $g(r)[O_W-H_{C2}]$ . These implies that the  $H_{C1}$  atom shows better capabilities in forming the weak  $C-H \cdots O$  contacts than the  $H_{C2}$  atom. The broad peaks of the RDFs also reveal that the intermolecular interactions are likely to include the weak hydrogen bonds as well as other weak interactions such as dipolar interactions and dispersions. So the weak  $C-H \cdots O$  contacts can not be neglected in glycylglycine-water mixtures even though the intensities of the weak  $C-H \cdots O$  contacts are weaker than those of the strong hydrogen bonds.

### B. Hydrogen-bonding network

As shown above, the different atoms show different capabilities in forming hydrogen bonds. But RDFs do not provide explicit information on ordering in binary mixtures, we carry out a detailed analysis of hydrogen bonding network in the mixtures to gain deeper insight into the aqueous structures. One basic aspect of the hydrogen bonding network is the probability distribution, describing the number and type of hydrogen bonds that a molecule is engaged in with other molecules. The hydrogen bonds are determined by a similar geometrical criterion to that of pure water as defined above. The statistics of  $C=O1 \cdots H_W$  hydrogen bonds,  $C=O2 \cdots H_W$ ,  $C=O2 \cdots H_W$ , and  $H_W-O_W \cdots H_W$  are given in Fig.3. It is found that the free carbonyl oxygen atoms are in the level of 15%–20% with concentration, and the fractions of cluster for the carbonyl oxygen atom accepting one protons of water ( $H_W$ ) are in high level (65%–70%) shown in Fig.3(a). These indicate that the aggregates of carbonyl oxygen atom accepting one protons is dominant in the hydrogen bonds of  $C=O1 \cdots H_W$ . However, the free carbonyl oxygen atoms in  $C=O2 \cdots H_W$  hydrogen bonds almost do not exist, shown in Fig.3(b). That is to say, nearly all the O2 atoms can form  $C=O \cdots H_W$  hydrogen bonds. The capability of O2 atom in forming hydrogen bonds is exactly stronger than that of O1 atom. There is just one

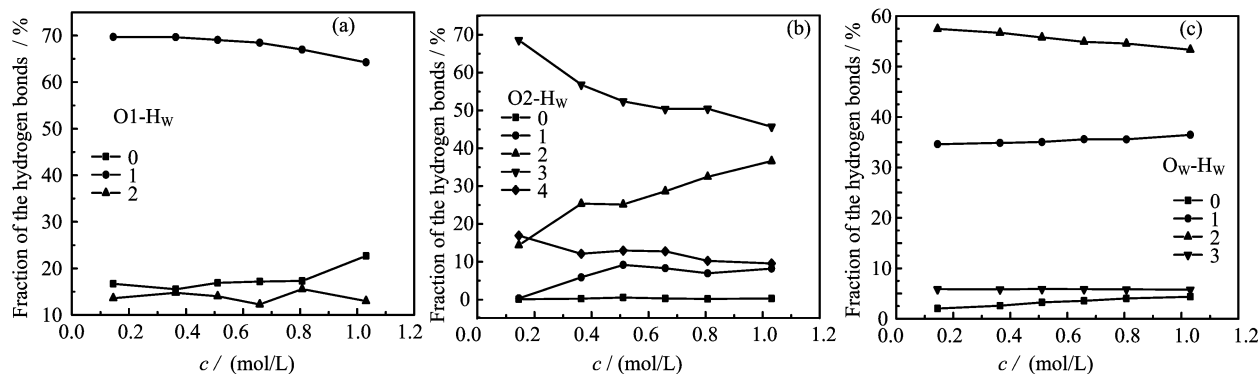


FIG. 3 Hydrogen-bonding network in glycyglycine-water system. (a) Fraction of O1 atoms accepting 0, 1, and 2 hydrogen bonds to H<sub>W</sub> atoms. (b) Fraction of O2 atoms accepting 0, 1, 2, 3, and 4 hydrogen bonds to H<sub>W</sub> atoms. (c) Fraction of O<sub>W</sub> atoms in water accepting 0, 1, 2, and 3 hydrogen bonds to H<sub>W</sub> atoms.

type accepting one protons in C=O1···H<sub>W</sub> hydrogen bonds. However, there are more types of aggregates observed in C=O2···H<sub>W</sub> hydrogen bonds in Fig.3(b). The clusters of carbonyl oxygen atom accepting two protons of water (H<sub>W</sub>) are in the highest level which shows this aggregates is dominant in C=O2···H<sub>W</sub> hydrogen bonds. Another aggregate of carbonyl oxygen atom accepting three protons of water (H<sub>W</sub>) is also noteworthy with fraction about 20%–30%. The more types of aggregates in C=O2···H<sub>W</sub> hydrogen bonds reveal that there are more water molecules surrounding the O2 atoms to form hydrogen bonds. The O2 atom are found to show better capabilities in forming C=O···H<sub>W</sub> than the O1 atom in RDF analysis. The statistical results also show the same cases as the RDFs. Water molecules can be both donors and acceptors of hydrogen bonds, leading ideally to tetrahedral water coordination. The statistics of H<sub>W</sub>–O<sub>W</sub>···H<sub>W</sub> hydrogen bonds are given in Fig.3(c). The aggregate of O<sub>W</sub> accepting two protons of water (H<sub>W</sub>) is in a high level which is the dominant structure in O<sub>W</sub>···H<sub>W</sub> hydrogen bonds. The carbonyl and the water oxygen atoms compete as acceptors of hydrogen bonds. Moreover, the water and the hydrogen atoms in glycyglycine compete as donors of hydrogen bonds. It is the competition of these hydrogen bonding interactions which lead to hydrogen bonding networks in the glycyglycine-water mixtures.

### C. Comparison with NMR experiment

Spectral measurements such as IR, Raman, and NMR are highly powerful techniques that can be used to investigate intermolecular interactions in solution. However, there is still a little spectral data over the whole composition range for binary mixtures, especially in aqueous mixtures. It is not easy to obtain accurate chemical shifts with concentration and temperature dependence. And the relative chemical shifts are proven to be a good way to solve the problem [23, 24].

TABLE II The varieties of the relative chemical shifts of H<sub>W</sub>, H<sub>N2</sub>, and H<sub>C1</sub> (ppm) with temperature (within 40 K) at different concentration.

<i>c</i> <sub>glygly</sub> /(mol/L)	$\Delta\Delta\delta_{H_W}$	$\Delta\Delta\delta_{H_{N_2}}$	$\Delta\Delta\delta_{H_{C_1}}$
0.151	−0.291	−0.202	−0.005
0.370	−0.290	−0.184	−0.005
0.519	−0.298	−0.207	−0.006
0.661	−0.312	−0.220	−0.003
0.812	−0.302	−0.211	−0.004
1.015	−0.302	−0.214	−0.003

It is well known that the effect of hydrogen bond on the chemical shift is much larger than all of the other intermolecular interaction effects. Hydrogen bonding interactions are also sensitive to temperature [15, 16, 23]. The variety of the chemical shifts in NMR can also reflect the change of the hydrogen bonds in the aqueous solution. The chemical shift moves to high field and the value becomes smaller with the temperature increasing. Strong hydrogen bond leads to greater shift than weak hydrogen bond.

The chemical shifts of H<sub>C2</sub> atom ( $\delta_{H_{C_2}}$ ) are used as a reference standard in the glycyglycine aqueous solution. The relative chemical shifts of water ( $\Delta\delta_{H_W}$ ), amide group ( $\Delta\delta_{H_{N_2}}$ ) and H<sub>C1</sub> atom ( $\Delta\delta_{H_{C_1}}$ ) with temperature are given in Fig.4. The relative chemical shifts of the three different hydrogen atoms all decrease with the temperature increasing which reveals that the hydrogen bonds interactions play important role in the aqueous solutions. However, the decreasing tendency of the three atoms exhibit different cases. The detailed data are given in Table II. The varieties of the relative chemical shifts of water hydrogen ( $\Delta\Delta\delta_{H_W} \approx 0.3$  ppm) are larger than those of amide hydrogen ( $\Delta\Delta\delta_{H_{N_2}} \approx 0.2$  ppm). These reveal that the capabilities in forming hydrogen bonds of H<sub>W</sub> atoms are stronger than the H<sub>N2</sub> atoms which are in agreement with the results in RDFs analysis. The C–H···O con-

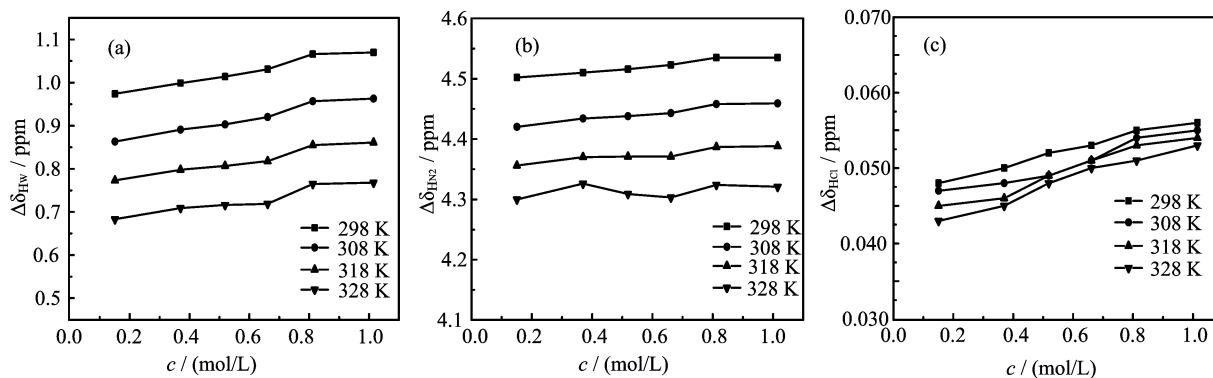


FIG. 4 Relative chemical shifts of different hydrogen atoms in glycylglycine aqueous solutions. (a) Hydrogen atoms in water, (b) hydrogen atoms in amide group, and (c)  $H_{C1}$  atom.

tact is weakest, so the varieties of the  $\Delta\delta_{H_{C1}}$ s are the smallest ( $\Delta\Delta\delta_{H_{C1}} \approx 0.005$  ppm). The relative  $\Delta\delta_{H_{C1}}$  decreases with temperature which imply that the  $H_{C1}$  atom is more favored in forming C–H $\cdots$ O weak contacts than the  $H_{C2}$  atom. The results show agreement with the MD simulations.

## V. CONCLUSION

An all-atom MD simulation combined the NMR experiment are performed to investigate the structures and interactions in the *N*-glycylglycine aqueous system. The results of RDF indicate that the different types of atoms exhibit different capability in forming hydrogen bonds. The O2 atoms show better capability in forming C=O $\cdots$ H<sub>W</sub> hydrogen bonds than O1 atoms. The H<sub>W</sub> favored in forming H $\cdots$ O<sub>W</sub>–H<sub>W</sub> rather than the H<sub>N2</sub> atoms. For the weak C–H $\cdots$ O contacts, the  $H_{C1}$  and  $H_{C2}$  atoms also exhibit different abilities in forming hydrogen bonds. Through the analysis for hydrogen-bonding network, some different typical dominant aggregates are found in the different types of hydrogen bonds. Nearly all the O2 atoms can form C=O $\cdots$ H<sub>W</sub> hydrogen bonds, the O2 atoms form C=O $\cdots$ H<sub>W</sub> hydrogen bonds, the O2 atoms are proven to be a better proton acceptor than the O1 atoms. The different hydrogen atoms are different which show good agreement with the results in the MD simulations. All-atom MD simulations and NMR spectra are successful in revealing the structures and interactions in the *N*-glycylglycine-water mixtures.

## VI. ACKNOWLEDGMENTS

This work was supported by the National Natural Science Foundation of China (No.20903026), the Science and Technology Planning Project of Guangdong Province (No.2007B030702007), the Faculty Construction Foundation of Guangdong Pharmaceutical Univer-

sity, the Foundation of the Science Instruments Cooperation of Guangzhou (No.2011010), and the Project for High-level Talents in Colleges of Guangdong Province.

- [1] A. Rath, D. V. Tulumello, and C. M. Deber, *Biochemistry* **48**, 3036 (2009).
- [2] L. A. Ralat, Y. Manevich, A. B. Fisher, and R. F. Colman, *Biochemistry* **45**, 360 (2006).
- [3] Y. S. Velichko, S. I. Stupp, and M. O. Cruz, *J. Phys. Chem. B* **112**, 2326 (2008).
- [4] R. Zhang, Z. Y. Tan, and S. L. Luo, *Chin. J. Chem. Phys.* **21**, 221 (2008).
- [5] A. Vallee, V. Humblot, and C. M. Pradier, *Acc. Chem. Res.* **43**, 1297 (2010).
- [6] R. Zhang, H. Li, Y. Lei, and S. Han, *J. Mol. Struct.* **693**, 17 (2004).
- [7] M. Chalaris and J. Samios, *J. Chem. Phys.* **112**, 8581 (2000).
- [8] T. Köddermann and R. Ludwig, *Phys. Chem. Chem. Phys.* **6**, 1867 (2004).
- [9] M. Jabłoński and A. J. Sadlej, *J. Phys. Chem. A* **111**, 3423 (2007).
- [10] D. Sheppard, D. Li, R. Godoy-Ruiz, R. B. Schweiler, and V. Tugarinov, *J. Am. Chem. Soc.* **132**, 7709 (2010).
- [11] B. A. Hall and M. S. P. Sansom, *J. Chem. Theory Comput.* **5**, 2465 (2009).
- [12] A. Khalfa and M. Tarek, *J. Phys. Chem. B* **114**, 2676 (2010).
- [13] A. Vishnyakov, A. P. Lyubartsev, and A. Laaksonen, *J. Phys. Chem. A* **105**, 1702 (2001).
- [14] J. Griffiths, *Anal. Chem.* **81**, 1725 (2009).
- [15] M. G. N. Reddy and S. Caldarelli, *Anal. Chem.* **82**, 3266 (2010).
- [16] K. Mizuno, S. Imafuji, T. Fujiwara, T. Ohta, and Y. Tamiya, *J. Phys. Chem. B* **107**, 3972 (2003).
- [17] K. Mizuno, S. Imafuji, T. Ochi, T. Ohta, and S. Maeda, *J. Phys. Chem. B* **104**, 11001 (2000).
- [18] L. Wang, M. Liu, L. Zhu, H. Li, D. Sun, and Y. Di, *J. Chem. Eng. Data* **54**, 2251 (2009).
- [19] O. B. Morozova and A. V. Yurkovskaya, *J. Phys. Chem. B* **112**, 12859 (2008).

- [20] V. Pajcini, X. G. Chen, R. W. Bormett, S. J. Geib, P. Li, S. A. Asher, and E. G. Lidiak, *J. Am. Chem. Soc.* **118**, 9716 (1996).
- [21] D. N. Kurhe, D. H. Dagade, J. P. Jadhav, S. P. Govindwar, and K. J. Patil, *J. Phys. Chem. B* **113**, 16612 (2009).
- [22] R. Zhang, D. Zheng, Y. Pan, S. Luo, and H. Li, *J. Mol. Struct.* **875**, 96 (2008).
- [23] R. Zhang, H. Li, Y. Lei, and S. Han, *J. Phys. Chem. B* **108**, 12596 (2004).
- [24] R. Zhang, H. Li, Y. Lei, and S. Han, *J. Phys. Chem. B* **109**, 7482 (2005).
- [25] H. J. C. Berendsen, J. P. M. Postma, W. F. van J. Gunsteren, and G. Hermans, *In Intermolecular Forces*, Reid: Dordrecht, 331 (1981).
- [26] W. L. Jorgensen, D. S. Maxwell, and J. Tirado-Rives, *J. Am. Chem. Soc.* **118**, 11225 (1996).
- [27] W. L. Jorgensen and C. Swenson, *J. Am. Chem. Soc.* **107**, 1489 (1985).
- [28] M. J. Dudek, K. Ramnarayan, and J. W. Ponder, *J. Comput. Chem.* **19**, 548 (1998).
- [29] A. Luzar and D. Chandler, *J. Chem. Phys.* **98**, 8160 (1993).
- [30] G. Zheng, T. Stait-Gardner, P. G. Anil Kumar, A. M. Torres, and W. S. Price, *J. Magn. Reson.* **191**, 159 (2008).
- [31] R. P. L. Clairac, B. H. Geierstanger, M. Mrksich, P. B. Dervan, and D. E. Wemmer, *J. Am. Chem. Soc.* **119**, 7909 (1997).
- [32] Q. Wang, W. Xu, Q. Xue, and W. Su, *J. Zhejiang Univ. Sci. B* **11**, 851 (2010).